



The success of emissions control legislation in mitigating air pollution is higher than previously estimated.

Nikos Daskalakis^{1,2,*}, Kostas Tsigaridis^{3,4}, Stelios Myriokefalitakis¹, George S. Fanourgakis¹, and Maria Kanakidou¹

¹Environmental Chemical Processes Laboratory, Department of Chemistry, University of Crete, P.O.Box, 2208, 70013 Heraklion, Greece

²Institute of Chemical Engineering, Foundation for Research and Technology Hellas (ICE-HT FORTH), 26504 Patras, Greece

³Center for Climate Systems Research, Columbia University, New York, NY 10025, USA

⁴NASA Goddard Institute for Space Studies, 2880 Broadway, New York, NY 10025, USA

* now at: LATMOS, Laboratoire Atmosphères, Milieux, Observations Spatiales, UPMC/UVSQ/CNRS, Paris, France

Correspondence to: Nikos Daskalakis: nick@chemistry.uoc.gr; Maria Kanakidou: mariak@chemistry.uoc.gr

Abstract.

During the last 30 years significant effort has been made to improve air quality through legislation for emissions reduction. Global three-dimensional chemistry-transport simulations of atmospheric composition changes over the past three decades have been performed to assess the impact of these measures. The simulations are based on assimilated meteorology to account for the year-to-year observed climate variability and on different anthropogenic emissions scenarios of pollutants which may or may not account for air quality legislation application. The ACCMIP dataset historical emissions are used as the starting point. We show that air quality legislation has been more efficient than thought in limiting the rapid increase of air pollutants due to significant technology development. The achieved reductions in nitrogen oxides, carbon monoxide, black carbon and sulphate aerosols are found to be significant when comparing to simulations neglecting legislation for the protection of the environment. We also show the large tropospheric air-quality benefit from the development of cleaner technology. These 30-year hindcast simulations demonstrate that the actual benefit in air quality due to air pollution legislation and technological advances is higher than the gain calculated by a simple comparison against a constant anthropogenic emissions simulation, as is usually done. Our results also indicate that over China and India the beneficial technological advances for the air-quality have been masked by the explosive increase in local population and the disproportional increase in energy demand.

15 1 Introduction

The rapid Earth's population increase that took place the last 60 years and the changes in human practices towards a society with larger energy consumption resulted in intensifying the atmospheric pollutant emission (Lamarque et al., 2013; Hand et al., 2012; Wang et al., 2014; Steffen et al., 2007). Air pollutants like ozone (O_3), carbon monoxide (CO), nitrogen oxides (NO_x), nitric acid (HNO_3) and particulate black carbon (BC), organic carbon (OC), sulphate (SO_4^{2-}) and nitrate (NO_3^-) have been observed to increase, reaching levels in the early 80's that threat ecosystems, leading for instance to agricultural efficiency decrease (Avnery et al., 2011) and human health inducing mortality increase (West et al., 2013), increase atmospheric acidity



(Likens et al., 1996) and affect climate (West et al., 2013). To limit the negative impacts of air pollution, aggressive measures have been taken in the 80's (Lamarque et al., 2013) to reduce human-induced emissions. In parallel, the growing number and accuracy of air quality observations enabled monitoring of the air quality changes and statistical association of such changes with health issues and other environmental impacts.

5 Pollutant levels and seasonal variation are closely connected to emissions of the pollutant or its precursors, and meteorology. Tropospheric ozone and aerosols have largely increased since pre-industrial times as a result of intense anthropogenic activity (Volz and Kley, 1988; Staehelin et al., 2001). Most anthropogenic activity takes place in the northern mid-latitudes with approximately 80% of global population residing there (Kummu and Varis, 2011). Thus the anthropogenically induced change in pollutant levels, hence in air quality, since pre-industrial times is expected to be larger in this area than in the southern hemisphere. Anthropogenic activity emitting NO_x into the atmosphere can influence the quantity of tropospheric ozone but because of ozone's non-linear dependency on the NO_x levels (Finlayson-Pitts and Pitts, 2000) the net effect on O_3 levels requires careful evaluation. Previous studies have shown that there is a 30% increase in the tropospheric ozone burden, that corresponds to 71 Tg, between 1890 and 1990 (Lamarque et al., 2005). This is linked to an increase of O_3 lifetime into the atmosphere by about 30% (Lamarque et al., 2005). Parrish et al. (2013) report a shift of 3–6 days in the seasonal cycle per decade for 15 the mid–northern latitudes, where most of the anthropogenic activity takes place, based on long continuous data records from monitoring sites in Europe. They attributed this shift to changes in the relative contribution of the different tropospheric O_3 sources, from the stratosphere, changes in large scale circulation and changes in O_3 precursor emissions and subsequent photochemical production within the troposphere. The springtime maximum in ozone concentrations in the Northern Hemisphere (N.H.) reflects the combination effect of increased free troposphere photochemical activity and stratospheric input (Vingarzan, 20 2004). In that work an increase of background ozone levels in the N.H. of 0.5–2% per year for the last 3 decades is reported, resulting to a mean concentration of 20–45 ppb for the N.H. for the year 2000. At Finokalia, Greece, Gerasopoulos et al. (2005) presented the changes in O_3 seasonality due to changes in meteorology and found a decreasing trend in ozone for the period 1997–2004 of about 1.64 ppb y^{-1} (3.1% y^{-1}). At the Mauna Loa observatory in Hawaii the 40–year timeseries of O_3 measurements shows that there is little change during spring but there is a rise during autumn, attributed to the weakening of the airflow from Eurasia in spring and strengthening in autumn (Lin et al., 2014). Oltmans et al. (2013) performed an extended analysis on long term (20–40 years) time series of global surface and ozonesonde observations. They found that the substantial tropospheric ozone increases observed in the early 1990s, the flattening, or even the decrease in ozone levels observed at several locations (e.g. Galcier NP, Minamitorishima) the past 10 years are results of the restrictions on precursor emissions. In the Southern Hemisphere subtropics a significant increase has also been observed (Oltmans et al., 2013). Similar findings were reported by Logan et al. (2012) by analysing measurements from sondes, aircraft and surface sites. These observations support the fact that O_3 variability depends on the geographical location (Chin, 2012) and the extent of regional anthropogenic influence (Vingarzan, 2004). The enhancements have levelled-off in the most recent decades, most probably due to O_3 precursors emissions control (Oltmans et al., 2013).

The global modelling study performed by Horowitz (2006) using the MOZART–2 model showed a 50% increase in ozone 35 burden calculated since pre-industrial times and a -6% to +43% change projected for 2100 using different emission scenarios.



In agreement with that study, Stevenson et al. (2006) analysis of multi model simulations of the future atmosphere has shown that, depending on the anthropogenic emissions, and in particular NO_x , the change in the tropospheric O_3 burden in 2030 compared to the 2000 levels can range between -5% (most optimistic scenario) and +15% (most pessimistic scenario).

Observations also show statistically significant trends in surface levels of atmospheric pollutants like CO (Yoon and Pozzer, 2014), sulphate (Hand et al., 2012) as well as the aerosol optical depth (AOD) that provides a measure of the interaction of aerosol atmospheric column content with radiation (Zhang and Reid, 2010; Karnieli et al., 2009). Global AOD over the ocean has been recorded by the Advanced Very High Resolution Radiometer (AVHRR) satellite instrument to increase from 1985 to 1990 and to decrease from 1994 to 2006 (Li et al., 2014). CO surface levels were observed to increase before 1990s (Khalil and Rasmussen, 1988) and decrease in recent years, due to a decrease in CO anthropogenic emissions (Novelli et al., 1994). MOPITT, AIRS, TES and IASI satellite instruments have recorded a decreasing trend in the total column of CO of about -1% per year in the northern hemisphere and less than that in the southern hemisphere from 2000 to 2011 (Worden et al., 2013).

In the troposphere all major air pollutants have sufficiently long lifetimes to be transported (Textor et al., 2006; Oltmans et al., 2013; Worden et al., 2013; Daskalakis et al., 2015). Thus, in addition to their precursor emissions and chemistry, atmospheric circulation is controlling air pollutant levels. Changes in transport patterns and spatial and temporal changes in anthropogenic emissions of O_3 precursors were suggested as the main causes of the observed shifts in seasonal maxima of O_3 in the northern hemisphere (Lin et al., 2014; Parrish et al., 2013) and the increase in wintertime levels of O_3 compared to earlier years (Parrish et al., 2013). Simulations suggest that the weakening of monsoon circulation in past decades contributed to the observed high aerosol levels in China (Chin, 2012), while a 6-year analysis of the Moderate Resolution Imaging Spectroradiometer (MODIS) AOD over the Mediterranean attributed to observed AOD changes to anthropogenic emissions during summertime and to changes in precipitation during wintertime (Papadimas et al., 2008).

Traditionally, air quality assessments are performed by comparing the pollutants concentrations at present with those of a past year. However, to evaluate the effectiveness of the applied legislation in air quality, we need to account for the changes induced by meteorology and the increase in anthropogenic emissions due to increase in population and energy demand.

For the present study, a set of three different interannual global three-dimensional chemistry transport simulations of atmospheric composition changes over the past three decades has been performed and analysed to assess the effectiveness of measures taken in the past years to limit air quality deterioration. The first simulation is performed using historical anthropogenic emissions and the second one using anthropogenic emissions as those of the year 1980. The third 30-year simulation represents the worst case scenario and is performed with anthropogenic emissions for the period 1980-2010 that have been constructed, as further explained, in order to account for population increase but not for the applied legislation since 1980.

2 Methodology – The global model setup

The model used for this work is the global 3D chemistry-transport model (CTM) TM4-ECPL (Kanakidou et al., 2012; Daskalakis et al., 2015) that takes into account gas and multiphase chemistry (Myriokefalitakis et al., 2011), gas-particle partitioning of semi volatile organics (Tsigaridis et al., 2006), and computed the gas-to-particle partitioning of inorganic com-



ponents and the aerosol water using the ISORROPIA II aerosol thermodynamic model (Fountoukis and Nenes, 2007) in which the dust components are neglected for the present study. TM4–ECPL low horizontal resolution of $4^\circ \times 6^\circ$ latitude by longitude and 34 hybrid vertical layers to 0.1 hPa was used here driven by ECMWF ERA–Interim meteorology from 1980 to 2010 (Dee et al., 2011).

5 TM4–ECPL model targets the simulation of tropospheric composition and chemistry. To be computationally efficient, the model has low vertical resolution in the stratosphere, and very primitive representation of the full set of stratospheric chemistry. For this reason TM4–ECPL forces the O_3 concentrations in the top 3 model layers (50hPa – 10hPa) based on the monthly mean observations by the Microwave Scanning Radiometer (MSR) satellite for the years 1980–2008 and Global Ozone Monitoring Experiment (GOME2) for the years 2009–2010. These data have been interpolated to the model layers by the Royal Netherlands
10 Meteorological Institute (KNMI) (van der A et al., 2010). TM4–ECPL also calculates nitric acid concentration based on O_3 levels using a ratio derived from Upper Atmosphere Research Satellite (UARS) at 10 hPa. To account for CH_4 oxidation in the stratosphere, the CH_4 concentrations in the top eight layers of the model (roughly above 17 km height) are forced to HALOE CH_4 climatology (Huijnen et al., 2010).

Since TM4–ECPL, like most CTM's, does not explicitly consider methane emissions, it forces the surface CH_4 distribution
15 to observations using the latitudinal monthly varying surface levels of CH_4 calculated by Dentener et al. (2003) for the year 1984, which correspond to a global mean surface concentration of 1.69 ppm. This surface concentration changes depending on the simulated year and following the measured increase of CH_4 in the atmosphere. For the years between 1979 and 1989, the CH_4 surface distribution of the year 1984 is scaled to fit the observed ice core CH_4 data of the respective year. For the years between 1990 and 2010 prescribed CH_4 surface concentration files based on National Oceanic and Atmospheric
20 Administration (NOAA) observations are used (M. van Weele, personal communication, 2013).

The oceanic emissions of aerosols and isoprene are calculated by the model based on the 3–h varying meteorology and on monthly varying chlorophyll (Myriokefalitakis et al., 2011; Vignati et al., 2010). Other VOC emissions from the ocean have been taken into account in the model using the POET database (Granier et al., 2003) and have been kept constant from year to year (Myriokefalitakis et al., 2010). Interannually and daily varying dust emissions are from AeroCom (Aerosol comparisons
25 between observations and models Dentener et al., 2006, extended by E. Vignati, personal communication, 2012) for years from 2000 to 2010 and have been also applied to earlier decades assuming the same interannual variability. Even though dust emissions are not representative for the first years of the simulation, none of the pollutants examined here are influenced by dust. Therefore, this model deficiency does not affect the present study. Monthly varying isoprene, terpenes and other biogenic volatile organic compounds for the years 1980–2010 are from the global emissions calculated by the Model of Emissions of
30 Gases and Aerosols from Nature (MEGANv.1) (Sindelarova et al., 2014). Lightning NO_x emissions are calculated online and soil emissions are climatological emissions from the POET database (Granier et al., 2003).

Monthly anthropogenic and biomass burning emissions for the hindcast historical simulation are from the Atmospheric Chemistry and Climate Model Intercomparison Project (ACCMIP) database (Lamarque et al., 2013) until the year 2000 and RCP6.0 (van Vuuren et al., 2011; Fujino et al., 2006) projections afterwards. As anthropogenic emissions in this paper we



consider the sectors included in the anthropogenic emissions of the ACCMIP database (Lamarque et al., 2013). International shipping and aircraft emissions are also from the ACCMIP database in all simulations.

2.1 Simulations performed

Three global chemistry–transport interannual simulations of atmospheric composition changes during the past 3 decades (1980–2010) were here performed using assimilated meteorology, natural emissions and biomass burning emissions specific of the simulated year. Only the anthropogenic emissions of pollutants were different between the simulations: The Current Legislation (CL) simulation uses the historical emissions of the ACCMIP database where legislation is applied to limit air pollution (Lamarque et al., 2013). The Anthropogenic Emissions 1980 (AE1980) simulation uses anthropogenic emissions that are constant throughout the years and equal to those of the year 1980. This corresponds to simulations that are typically used for comparison when evaluating the efficiency of emission control scenarios. The Business As 1980 (BA1980) simulation accounts for constant anthropogenic emissions per capita and per HTAP region, as of the year 1980, resulting in anthropogenic emissions which follow the observed population changes (World Development Indicators, The World Bank; <http://www.worldbank.org/>). In this simulation the anthropogenic emissions neglect the air pollution legislation applied for emission mitigation after 1980. It does not account neither for the technological improvements achieved since 1980 nor for the per capita energy demand changes (Table S2). Finally, an extra simulation was performed identical to the CL simulation but using the fine resolution of the model ($3^\circ\text{lon} \times 2^\circ\text{lat}$) in order to investigate the effect of the model resolution on the results.

2.2 Construction of the BA1980 anthropogenic emissions

The BA1980 inventory assumes that land anthropogenic emissions per capita remained constant from 1980 until now in major geographic regions, while population and thus overall human driven emissions changed. Advances in technologies as well as increases in energy demand per capita have been assumed to have remained unchanged with time. To construct this anthropogenic emissions database the ACCMIP anthropogenic emissions of the year 1980 together with global population maps were used.

The global population for the year 1980 (not gridded) and global gridded population maps for the period 1990–2010, available at five–year increments were obtained from the United Nations (<http://www.un.org/>) and The World Bank (<http://www.worldbank.org/>). Using a fine resolution of $1^\circ \times 1^\circ$, linear interpolation between the 5–year steps was applied per grid to produce global gridded population density maps for each year for the period 1990–2010. The gridded population maps for the years 1980–1989 were subsequently constructed based on the gridded population distribution of the year 1990 and a backwards extrapolation of the year–to–year change of the total global population using a polynomial fit, thus assuming uniform population change in all regions.

Figure S1 provides a visual representation of the 16 regions considered in this study which correspond to the HTAP source regions (Janssens-Maenhout et al., 2015). Emission factors per species per capita per year for each HTAP source region were calculated for the year 1980 by dividing the 1980 anthropogenic emissions by the population of each region. These factors were then applied on the gridded population maps to construct the database of annually–varying BA1980 anthropogenic emissions.



Based on the population density, the anthropogenic land emissions of 1980 and the source regions as socio-economic regions, an emission inventory has been created that takes into account the per capita anthropogenic emissions of 1980, the population density increase per grid for the period 1980-2010 and the population relocation since 1990. As a result, a worst-case anthropogenic emission inventory was constructed, which assumes non-mitigation for improvement of air quality after 1980 and does not account neither for technological developments since then nor for increases in energy demand per capita but accounts for population increase. Increase in energy demand per capita is almost negligible in Europe and N. America but is significant in the fast developing countries, India and China (a factor of 2 and 3 respectively, Table S2b).

3 Results and discussion

3.1 Emission Trends

In Fig. 1, the annual mean anthropogenic emissions for the CL (historical changes) and the BA1980 emission scenarios for CO, NO_x, NH₃, OC, BC and SO₂ are presented, normalized to the respective emissions of the year 1980 (fluxes for the year 1980 are shown in the histograms in the same figure) for the considered regions: globe, Europe, N. America, China and India. During the entire 1980-2010 period the CL anthropogenic emissions of primary pollutants are lower than the BA1980 on the global scale and regionally over North America and Europe (Fig. 1 showing global and regional totals, and Fig. S2 and S3 showing gridded changes of the emissions). This demonstrates that effective emission controls and new technologies (CL emissions) have contributed to the reduction of air pollutants emissions, in a per-capita basis compared to those in 1980, resulting to overall reductions in anthropogenic emissions by 18% for BC to 44% for SO_x (sum of SO₂ and sulphate) globally and between 25% for NH₃ over N. America and 75% for SO_x over Europe (Table S2a) where most development of cleaner technologies was implemented. Energy demand per capita remained constant in the European Union while that over North America decreased by about 10% according to World Bank statistics (Table S2). On the other hand, regions which experience fast population and economic growth in the last three decades (such as China and India) are calculated to have higher anthropogenic emissions under the CL scenario than under the BA1980 scenario (by 60% and 55% for NO_x, respectively, and by 25% and 135% for SO_x, respectively, Table S2a). This means that their anthropogenic emissions per capita have increased in the last 3 decades, resulting in a “dirtier” case from what one might had expected. It is obvious though that efforts have been made to reduce pollution over India the past 10 years, where anthropogenic emissions of CO, BC and OC show stability, or even decreasing trends.

During the last 30 years the industrial sector in Asia has experienced an explosive growth, resulting in a disproportional increase compared to the local population growth. Globalization and cheap labour led a large fraction of the world’s industrial production to occur over the greater India and China regions, in response to the global population and energy demand growth, not just the local one, which explains the increased per-capita emissions over these regions (CL compared to BA1980). Indeed, as reported by the World Bank, the energy demand per capita has increased by factors of about 2 to 3 for India and China, respectively, derived as the ratio of the energy demand per capita in 2010 to that in 1980. However, when comparing CL to BA1980 emissions for India and China most emission ratios are lower than the corresponding increase in the energy use per



capita. The CL to BA1980 comparison indicates that some improvements in air quality have been achieved in these countries during the recent years although they can not be seen in the interannual trends of the CL emissions over these regions that show emission increases. Emission mitigation can be detected in the CL scenario by the 25% – 70% reduction of all major pollutant emissions over India and China, except SO_x over India (Fig. 1f), compared to regional emissions estimates that account for mean increase in energy demand (Table S2b). Ammonia emissions present a more complicated pattern (Fig. 1c), as a result of the absence of any legislation on NH_3 emissions (Lamarque et al., 2013) and high uncertainty on ammonia emissions from India (Sharma et al., 2008).

3.2 Comparison against surface measurements

The accuracy of the model is evaluated by comparison with available observations around the globe (see locations in Fig. S4). Surface observations for O_3 and CO were obtained from the World Data Centre for Greenhouse Gases (WDCGG; <http://ds.data.jma.go.jp/gmd/wdcgg/introduction.html>). Surface observations of O_3 , BC and SO_4^{2-} over Europe and the U.S.A. were obtained from the European Monitoring and Evaluation Programme (EMEP; <http://www.emep.int>) and the Interagency Monitoring of Protected Visual Environments (IMPROVE; <http://vista.cira.colostate.edu/improve/>) respectively. The OC measurements are from the AeroCom Phase II database (Tsigaridis et al., 2014). Monthly mean and standard deviation are calculated from the original datasets available at various temporal resolutions. These datasets provide adequate coverage over Europe and N. America. For the rest of the globe, the temporal and spacial variability of the measurements is scattered, resulting in a model evaluation which is highly biased by N. America and Europe.

Surface concentrations and trends were calculated for each of the three scenarios to compare the computed atmospheric composition changes during the studied period. CL simulations have been compared to global observations of O_3 , CO, SO_4^{2-} , BC and OC (Fig. 2, Fig. 3 and supplementary figures S5 to S10). These comparisons are performed on monthly mean basis for all stations and all years from 1980 to 2010 where data are available. Statistical analysis of the results was conducted per model grid. For this, monthly mean of the measurements were grouped per model grid ($6^\circ \times 4^\circ$ or $3^\circ \times 2^\circ$ depending on model resolution) and they are then averaged to derive the annual mean concentration. Model results are sampled at the time and location of the observations, then annual means in each grid box are computed for model results and compared to those derived from observations. The statistics of these comparisons are presented in Table 1.

In the following we focus on the normalized mean bias (NMB) to evaluate the over/underestimation of the observations by the model as well as the correlation coefficient that provides the strength and direction of the relationship between the model results and the observed levels of air pollutants, while the coefficient of determination (R^2) provides the fraction of the observed air pollutant variance that is reproduced by the model. In Table 1 that summarizes the statistics of Fig. 3, it can be seen that at the studied locations where observations are available the model reproduces very well the mean observed surface levels of CO (NMB between -1% and 2% for fine and coarse model resolution, respectively) and of BC (NMB between 1% and -3% for fine and coarse model resolution, respectively). It also satisfactorily reproduces the surface O_3 levels (NMB between 17% and 13% for fine and coarse model resolution, respectively). For sulfate the NMB is of the order of 61% and 52% respectively, indicating a model overestimate of the observations, while for particulate OC, the negative NMB between -57% and -62%



respectively indicates a model underestimate of the surface OC observations as also pointed out for most AeroCom models by Tsigaridis et al. (2014). The model performance is not as good for NH_4^+ aerosol which is overestimated by the model by a factor of about 1.4 to 1.5. The model results show relatively weak correlations with O_3 and CO observations ($0.4 < R < 0.5$) and very good correlations ($R > 0.5$) with the other air pollutants (Table 1). However, when focusing on the model's ability to reproduce the measured patterns as determined by the coefficient of determination (R^2), the model seems to capture nicely the observed variance of sulfates and OC with $R^2 > 0.5$, i.e. more than 50% of the observed variability is reproduced by the model. It also reproduces more than 40% of the observed NH_4^+ variability, 50% of that of BC, 25% of that of O_3 and about 20% of that of CO.

When further analyzing the model results to evaluate the success of applied legislation for improving air quality, we need to take into account the above outlined model's ability in reproducing observed air pollutant trends. For that, we used available monitoring stations with long timeseries of measurements (Fig. 2 and supplementary Figures S5-S10). For each of these stations the trends from the observations and from the corresponding values calculated by each simulation were derived. The model reproduces the sign of the observed trend for most species and locations. Specifically, SO_4^{2-} slope direction is always captured by the model, although the magnitude is not always well reproduced. O_3 and CO trends are also nicely well simulated, both in direction and in magnitude in most stations. OC, BC and NH_4^+ calculations appear to have the largest deviations from the trends derived from observations, which reflects the difficulties both in measuring carbonaceous and ammonium aerosols and in simulating their sources and fate in the atmosphere, in particular the semi volatile character of a large fraction of organics and of ammonium nitrate.

3.3 Impact of the model resolution on the calculated results

To determine the impact of the model resolution to the calculated results, an extra 30-year long simulation was performed identical to the CL simulation but using a finer model resolution of $3^\circ\text{lon} \times 2^\circ\text{lat}$. The calculated normalized annual mean concentrations of this simulation are depicted by the yellow line in Fig. 4. Also, statistical analysis identical to the one of the CL simulation was performed. The results of this analysis are also provided in Table 1 and shown in Fig. S11.

The statistical analysis of the comparison of the CL-fine simulation against measured values shows a global performance very similar to that of the CL simulation, indicating that, for the studied period and pollutants, the model resolution has only minor impact on the results. The largest differences in performance between the fine and coarse grid CL simulations are found for O_3 , where the calculated model mean value for the CL-fine simulation is about 4% higher than that of the CL simulation. Note that the differences in the model resolution reflect also in differences in the number of observational sites per grid and in the mean of the observed concentrations that are compared to the model results. These differences also reflect the inhomogeneity in the spatial coverage of the observations. When using finer resolution grids, the largest differences in the mean concentrations (Table 1), have been computed for the aerosol components and in particular for OC ($2.92 \mu\text{g m}^{-3}$ compared to $3.24 \mu\text{g m}^{-3}$, i.e. 10% lower compared to the coarse resolution grid). These differences are in accordance with the changes in the normalized mean simulated concentrations that are shown in Fig. 4.



3.4 Air quality changes

Because the CL, BA1980 and AE1980 simulations have been performed using the same meteorological fields, natural and biomass burning emissions, and differ only in the anthropogenic emissions over land, the effectiveness of the applied mitigation policies can be evaluated by comparison of the computed annual mean surface concentrations of air pollutants (Fig. 2, 3 and 5 supplementary figures S5 to S10 and Table S3).

The results are analysed by examining the changes in the computed concentrations in 2010 compared to the concentrations in 1980 as well as the percent changes between the different simulations in 2010. Focus is put on developed areas where mitigation legislation was applied (North America and Europe) and contrasting with India and China that experienced rapid growth during the last years. The AE1980 simulation shows a small variability (maximum 20%, usually about 5%) in the 10 normalized mean concentrations of pollutants (Fig. 4) that can be attributed to the climate variability in meteorology and the natural and biomass burning emissions. In Fig. 4, it is clearly seen that the climate impact on surface concentrations of O₃, OC and BC results in increases in their levels by about 5%, 15% and 5% respectively, in 2010 compared to 1980 on the global scale and also over Europe, North America and China, indicating that natural emissions are also significant there. The other pollutants in Fig. 4 show less sensitivity to meteorological and biomass burning changes.

15 Focusing on the CL simulation, small global decreases are computed for CO and SO₄²⁻ in 2010 (about -5% and -15%, respectively) since 1980, while for the other pollutants global increases are calculated (Fig. 4 left column). Regionally the picture is quite different, with significant reductions in primary pollutants over Europe and North America (except NO_x) and increases over China and India. For surface CO the environmental gain is substantial for Europe and for North America, with simulated reductions reaching -40% and -20% compared to the AE1980 levels (Fig. 4 green lines compared to blue lines), 20 while the large increase in energy use in China resulted in about 20% increase in surface CO.

The present study shows that the effectiveness of air pollution abatement is larger than what is deduced by comparing CL to AE1980 (Table S3a), as is usually done since comparisons of the CL simulation with the BA1980 one (that takes into account the population changes but neglects any technological developments since 1980, Table S3b) reveal a higher gain in air quality. Globally the computed surface CO levels under the CL simulation are lower than the BA1980 ones by 22%. Regionally the 25 reductions achieved in 2010 are even higher (Europe -69%, N. America -44%, China -19%, India -24%). This proves that technological advances of the past years have contributed to reduce the CO levels even in fast developing countries. These agree with changes in the total CO columns retrieved from satellite observations where reductions of the total column of CO are observed for all the studied regions for the period from 2000–2010 (Worden et al., 2013).

Another successful story is that of SO₄²⁻. Compared to the BA1980, SO₄²⁻ levels computed by the CL simulation are 30 lower by 54% globally, and more than a factor of 3 over Europe and almost a factor of 2 over N. America. In contrast, in the fast developing economies of China and India, computed SO₄²⁻ levels are higher by about 10%. However, if we account for the increase in energy demand per capita in these regions (by factors of 3 for China and 2 for India) that is not taken into consideration when constructing the BA1980 emissions database, then technological advances seem to have limited the air pollution even in these regions (Table S2b). The computed increase in surface SO₄²⁻ levels over China until about 2007 followed



by a stabilization and even a decrease in their levels, is in general agreement with the SO₂ column satellite observations (GOME/SCIAMACHY) that show increases between 1996 and 2007 and then a decrease in SO₂ tropospheric column over China (SCIAMACHY Product Handbook).

For OC and BC, the global gain computed is 10% and 22% respectively. Regionally, Europe shows the highest gain with a
5 computed reduction of OC of 54% and BC of 66%. N. America also shows high computed air quality gains concerning OC
and BC, with a 43% and 51% reduction respectively. For India a gain of 20% is computed for both pollutants, where for China
the changes are not significant (less than 5% for both).

Ozone levels show the least sensitivity to the reduction policies of its precursors' emissions, with computed global/regional
changes of less than 10%. These model results are also supported by the small zonal changes (between $-0.2 \pm 0.4\%$ y⁻¹,
10 $0.3 \pm 0.4\%$ y⁻¹) in tropospheric ozone column retrieved from SCIAMACHY observations between 2003 and 2011 (Ebojie
et al., 2015). Surface NO_x concentrations show increases by 13% and 28% over India and China respectively in the CL
compared to the BA1980 simulation while over Europe a reduction of 63% and over N. America of 29% is computed, where
the global gain is 21%. These results are in general agreement with the satellite observations by Richter et al. (2005), according
to which the tropospheric columns of NO_x are found to be rather stable or with a decreasing trend over Europe and the U.S.A.,
15 while they show an increasing trend over the Asian regions they studied during the period between 1996 and 2002.

4 Conclusions

Over the last century increasing population and technology development are modifying Earth's landscape, depleting resources
and changing the atmospheric composition, thus, deteriorating the quality of life on Earth. During the last 30 years significant
effort has been made to improve air quality through legislation for emissions reduction. The extent of success of the legislation
20 applied to improve air quality has been here assessed based on three global three-dimensional chemistry transport simulations
of atmospheric composition changes which were performed using different anthropogenic emissions of pollutants which may
or may not account for air quality legislation application. Otherwise identical, the simulations account for the year-to-year
observed climate and natural emissions variability. Air quality legislation has been shown to be more efficient than thought
in limiting the rapid increase of air pollutants due to significant technology development. The achieved reductions in nitrogen
25 oxides (21%), carbon monoxide (22%), black carbon (22%) and sulphate aerosols (54%) are found to be significant when
compared to simulations that neglect legislation for the protection of the environment and when taking into account the limits
of the model to reproduce the variance of the observations and the observed trends as earlier discussed. We also show the
large environmental benefit from the development of cleaner technology. Our 30-year hindcast simulations demonstrate that
the actual benefit in air quality due to air pollution legislation and technological advances is higher than the gain calculated by
30 a simple comparison against a constant anthropogenic emissions simulation, as is usually done. Our results also indicate that
over China and India the beneficial technological advances for the environment have been masked by the explosive increase in
local population and the disproportional increase in energy demand.



Acknowledgements. This work has been supported by the EU-FP7 project PEGASOS (FP7-ENV-2010-265148), the EU-FP7 project ECLIPSE (FP7-ENV-2011-282688) and the EU-FP7 project BACCHUS (project number 603445). We thank Frank Dentener and Michael Gauss for pertinent comments during early stages of this work.



References

- Avnery, S., Mauzerall, D. L., Liu, J., and Horowitz, L. W.: Global crop yield reductions due to surface ozone exposure: 1. Year 2000 crop production losses and economic damage, *Atmospheric Environment*, 45, 2284–2296, doi:<http://dx.doi.org/10.1016/j.atmosenv.2010.11.045>, <http://www.sciencedirect.com/science/article/pii/S1352231010010137>, 2011.
- 5 Chin, M.: Atmospheric science: Dirtier air from a weaker monsoon, *Nature Geosci*, 5, 449–450, doi:10.1038/ngeo1513, <http://dx.doi.org/10.1038/ngeo1513>, 2012.
- Daskalakis, N., Myriokefalitakis, S., and Kanakidou, M.: Sensitivity of tropospheric loads and lifetimes of short lived pollutants to fire emissions, *Atmospheric Chemistry and Physics*, 15, 3543–3563, doi:10.5194/acp-15-3543-2015, <http://www.atmos-chem-phys.net/15/3543/2015/>, 2015.
- 10 Dee, D. P., Uppala, S. M., Simmons, A. J., Berrisford, P., Poli, P., Kobayashi, S., Andrae, U., Balmaseda, M. A., Balsamo, G., Bauer, P., Bechtold, P., Beljaars, A. C. M., van de Berg, L., Bidlot, J., Bormann, N., Delsol, C., Dragani, R., Fuentes, M., Geer, A. J., Haimberger, L., Healy, S. B., Hersbach, H., Hólm, E. V., Isaksen, I., Kållberg, P., Köhler, M., Matricardi, M., McNally, A. P., Monge-Sanz, B. M., Morcrette, J.-J., Park, B.-K., Peubey, C., de Rosnay, P., Tavolato, C., Thépaut, J.-N., and Vitart, F.: The ERA-Interim reanalysis: configuration and performance of the data assimilation system, *Quarterly Journal of the Royal Meteorological Society*, 137, 553–597, doi:10.1002/qj.828, <http://dx.doi.org/10.1002/qj.828>, 2011.
- 15 Dentener, F., van Weele, M., Krol, M., Houweling, S., and van Velthoven, P.: Trends and inter-annual variability of methane emissions derived from 1979–1993 global CTM simulations, *Atmospheric Chemistry and Physics*, 3, 73–88, doi:10.5194/acp-3-73-2003, <http://www.atmos-chem-phys.net/3/73/2003/>, 2003.
- Dentener, F., Kinne, S., Bond, T., Boucher, O., Cofala, J., Generoso, S., Ginoux, P., Gong, S., Hoelzemann, J. J., Ito, A., Marelli, L., Penner, J. E., Putaud, J.-P., Textor, C., Schulz, M., van der Werf, G. R., and Wilson, J.: Emissions of primary aerosol and precursor gases in the years 2000 and 1750 prescribed data-sets for AeroCom, *Atmospheric Chemistry and Physics*, 6, 4321–4344, doi:10.5194/acp-6-4321-2006, <http://www.atmos-chem-phys.net/6/4321/2006/>, 2006.
- 20 Ebojje, F., Burrows, J. P., Gebhardt, C., Ladstätter-Weissenmayer, A., von Savigny, C., Rozanov, A., Weber, M., and Bovensmann, H.: Global and zonal tropospheric ozone variations from 2003–2011 as seen by SCIAMACHY, *Atmospheric Chemistry and Physics Discussions*, 15, 24 085–24 130, doi:10.5194/acpd-15-24085-2015, <http://www.atmos-chem-phys-discuss.net/15/24085/2015/>, 2015.
- 25 Finlayson-Pitts, J. N. and Pitts, B. J.: *Chemistry of the Upper and Lower Atmosphere*, Academic Press, San Diego, doi:<http://dx.doi.org/10.1016/B978-012257060-5/50025-3>, 2000.
- Fountoukis, C. and Nenes, A.: ISORROPIA II: a computationally efficient thermodynamic equilibrium model for K^+ – Ca^{2+} – Mg^{2+} – NH_4^+ – Na^+ – SO_4^{2-} – NO_3^- – Cl^- – H_2O aerosols, *Atmospheric Chemistry and Physics*, 7, 4639–4659, doi:10.5194/acp-7-4639-2007, <http://www.atmos-chem-phys.net/7/4639/2007/>, 2007.
- 30 Fujino, J., Nair, R., Kainuma, M., Masui, T., and Matsuoka, Y.: Multi-gas Mitigation Analysis on Stabilization Scenarios Using Aim Global Model, *The Energy Journal*, Multi-Greenhouse Gas Mitigation and Climate Policy, 343–354, http://EconPapers.repec.org/RePEc:ajen:journl:2006se_weyant-a17, 2006.
- Gerasopoulos, E., Kouvarakis, G., Vrekoussis, M., Kanakidou, M., and Mihalopoulos, N.: Ozone variability in the marine boundary layer of the eastern Mediterranean based on 7-year observations, *Journal of Geophysical Research: Atmospheres*, 110, n/a–n/a, doi:10.1029/2005JD005991, <http://dx.doi.org/10.1029/2005JD005991>, d15309, 2005.



- Granier, C., Guenther, A., Lamarque, J., Mieville, A., Muller, J. F., Olivier, J., Orlando, J., Peters, J., Petron, G., Tyndall, G., and Wallens, S.: POET, a database of surface emissions of ozone precursors: Present and Future surface emissions of anthropogenic compounds, Tech. Rep. EVK2-1999-00011, EU, 2003.
- Hand, J. L., Schichtel, B. A., Malm, W. C., and Pitchford, M. L.: Particulate sulfate ion concentration and SO₂ emission trends in the United States from the early 1990s through 2010, *Atmospheric Chemistry and Physics*, 12, 10 353–10 365, doi:10.5194/acp-12-10353-2012, <http://www.atmos-chem-phys.net/12/10353/2012/>, 2012.
- Horowitz, L. W.: Past, present, and future concentrations of tropospheric ozone and aerosols: Methodology, ozone evaluation, and sensitivity to aerosol wet removal, *Journal of Geophysical Research: Atmospheres*, 111, n/a–n/a, doi:10.1029/2005JD006937, <http://dx.doi.org/10.1029/2005JD006937>, d22211, 2006.
- Huijnen, V., Williams, J., van Weele, M., van Noije, T., Krol, M., Dentener, F., Segers, A., Houweling, S., Peters, W., de Laat, J., Boersma, F., Bergamaschi, P., van Velthoven, P., Le Sager, P., Eskes, H., Alkemade, F., Scheele, R., Nédélec, P., and Pätz, H.-W.: The global chemistry transport model TM5: description and evaluation of the tropospheric chemistry version 3.0, *Geoscientific Model Development*, 3, 445–473, doi:10.5194/gmd-3-445-2010, <http://www.geosci-model-dev.net/3/445/2010/>, 2010.
- Janssens-Maenhout, G., Crippa, M., Guizzardi, D., Dentener, F., Muntean, M., Pouliot, G., Keating, T., Zhang, Q., Kurokawa, J., Wankmüller, R., Denier van der Gon, H., Kuenen, J. J. P., Klimont, Z., Frost, G., Darras, S., Koffi, B., and Li, M.: HTAP v2.2: a mosaic of regional and global emission grid maps for 2008 and 2010 to study hemispheric transport of air pollution, *Atmospheric Chemistry and Physics*, 15, 11 411–11 432, doi:10.5194/acp-15-11411-2015, <http://www.atmos-chem-phys.net/15/11411/2015/>, 2015.
- Kanakidou, M., Duce, R. A., Prospero, J. M., Baker, A. R., Benitez-Nelson, C., Dentener, F. J., Hunter, K. A., Liss, P. S., Mahowald, N., Okin, G. S., Sarin, M., Tsigaridis, K., Uematsu, M., Zamora, L. M., and Zhu, T.: Atmospheric fluxes of organic N and P to the global ocean, *Global Biogeochemical Cycles*, 26, n/a–n/a, doi:10.1029/2011GB004277, <http://dx.doi.org/10.1029/2011GB004277>, gB3026, 2012.
- Karnieli, A., Derimian, Y., Indoitu, R., Panov, N., Levy, R. C., Remer, L. A., Maenhaut, W., and Holben, B. N.: Temporal trend in anthropogenic sulfur aerosol transport from central and eastern Europe to Israel, *Journal of Geophysical Research: Atmospheres*, 114, n/a–n/a, doi:10.1029/2009JD011870, <http://dx.doi.org/10.1029/2009JD011870>, d00D19, 2009.
- Khalil, M. A. K. and Rasmussen, R. A.: Carbon monoxide in the Earth's atmosphere: indications of a global increase, *Nature*, 332, 242–245, doi:10.1038/332242a0, <http://dx.doi.org/10.1038/332242a0>, 1988.
- Kummu, M. and Varis, O.: The world by latitudes: A global analysis of human population, development level and environment across the north–south axis over the past half century, *Applied Geography*, 31, 495 – 507, doi:<http://dx.doi.org/10.1016/j.apgeog.2010.10.009>, <http://www.sciencedirect.com/science/article/pii/S0143622810001244>, 2011.
- Lamarque, J.-F., Hess, P., Emmons, L., Buja, L., Washington, W., and Granier, C.: Tropospheric ozone evolution between 1890 and 1990, *Journal of Geophysical Research: Atmospheres*, 110, n/a–n/a, doi:10.1029/2004JD005537, <http://dx.doi.org/10.1029/2004JD005537>, d08304, 2005.
- Lamarque, J.-F., Shindell, D. T., Josse, B., Young, P. J., Cionni, I., Eyring, V., Bergmann, D., Cameron-Smith, P., Collins, W. J., Doherty, R., Dalsoren, S., Faluvegi, G., Folberth, G., Ghan, S. J., Horowitz, L. W., Lee, Y. H., MacKenzie, I. A., Nagashima, T., Naik, V., Plummer, D., Righi, M., Rumbold, S. T., Schulz, M., Skeie, R. B., Stevenson, D. S., Strode, S., Sudo, K., Szopa, S., Voulgarakis, A., and Zeng, G.: The Atmospheric Chemistry and Climate Model Intercomparison Project (ACCMIP): overview and description of models, simulations and climate diagnostics, *Geoscientific Model Development*, 6, 179–206, doi:10.5194/gmd-6-179-2013, <http://www.geosci-model-dev.net/6/179/2013/>, 2013.



- Li, J., Carlson, B. E., and Laciš, A. A.: Revisiting AVHRR tropospheric aerosol trends using principal component analysis, *Journal of Geophysical Research: Atmospheres*, 119, 3309–3320, doi:10.1002/2013JD020789, <http://dx.doi.org/10.1002/2013JD020789>, 2013JD020789, 2014.
- Likens, G. E., Driscoll, C. T., and Buso, D. C.: Long-Term Effects of Acid Rain: Response and Recovery of a Forest Ecosystem, *Science*, 5 272, 244–246, doi:10.1126/science.272.5259.244, <http://www.sciencemag.org/content/272/5259/244.abstract>, 1996.
- Lin, M., Horowitz, L. W., Oltmans, S. J., Fiore, A. M., and Fan, S.: Tropospheric ozone trends at Mauna Loa Observatory tied to decadal climate variability, *Nature Geosci*, 7, 136–143, <http://dx.doi.org/10.1038/ngeo2066>, article, 2014.
- Logan, J. A., Staehelin, J., Megretskaia, I. A., Cammas, J.-P., Thouret, V., Claude, H., De Backer, H., Steinbacher, M., Scheel, H.-E., Stübi, R., Fröhlich, M., and Derwent, R.: Changes in ozone over Europe: Analysis of ozone measurements from sondes, regular aircraft 10 (MOZAIC) and alpine surface sites, *Journal of Geophysical Research: Atmospheres*, 117, n/a–n/a, doi:10.1029/2011JD016952, <http://dx.doi.org/10.1029/2011JD016952>, d09301, 2012.
- Myriokefalitakis, S., Vignati, E., Tsigaridis, K., Papadimas, C., Sciare, J., Mihalopoulos, N., Facchini, M. C., Rinaldi, M., Dentener, F. J., Ceburnis, D., Hatzianastasiou, N., O'Dowd, C. D., van Weele, M., and Kanakidou, M.: Global Modeling of the Oceanic Source of Organic Aerosols, *Advances in Meteorology*, 2010, doi:10.1155/2010/939171, 2010.
- 15 Myriokefalitakis, S., Tsigaridis, K., Mihalopoulos, N., Sciare, J., Nenes, A., Kawamura, K., Segers, A., and Kanakidou, M.: In-cloud oxalate formation in the global troposphere: a 3-D modeling study, *Atmospheric Chemistry and Physics*, 11, 5761–5782, doi:10.5194/acp-11-5761-2011, <http://www.atmos-chem-phys.net/11/5761/2011/>, 2011.
- Novelli, P. C., Masarie, K. A., Tans, P. P., and Lang, P. M.: Recent Changes in Atmospheric Carbon Monoxide, *Science*, 263, 1587–1590, doi:10.1126/science.263.5153.1587, <http://www.sciencemag.org/content/263/5153/1587.abstract>, 1994.
- 20 Oltmans, S., Lefohn, A., Shadwick, D., Harris, J., Scheel, H., Galbally, I., Tarasick, D., Johnson, B., Brunke, E.-G., Claude, H., Zeng, G., Nichol, S., Schmidlin, F., Davies, J., Cuevas, E., Redondas, A., Naoe, H., Nakano, T., and Kawasato, T.: Recent tropospheric ozone changes – A pattern dominated by slow or no growth, *Atmospheric Environment*, 67, 331 – 351, doi:<http://dx.doi.org/10.1016/j.atmosenv.2012.10.057>, <http://www.sciencedirect.com/science/article/pii/S1352231012010394>, 2013.
- Papadimas, C. D., Hatzianastasiou, N., Mihalopoulos, N., Querol, X., and Vardavas, I.: Spatial and temporal variability in aerosol properties 25 over the Mediterranean basin based on 6-year (2000–2006) MODIS data, *Journal of Geophysical Research: Atmospheres*, 113, n/a–n/a, doi:10.1029/2007JD009189, <http://dx.doi.org/10.1029/2007JD009189>, d11205, 2008.
- Parrish, D. D., Law, K. S., Staehelin, J., Derwent, R., Cooper, O. R., Tanimoto, H., Volz-Thomas, A., Gilge, S., Scheel, H.-E., Steinbacher, M., and Chan, E.: Lower tropospheric ozone at northern midlatitudes: Changing seasonal cycle, *Geophysical Research Letters*, 40, 1631–1636, doi:10.1002/grl.50303, <http://dx.doi.org/10.1002/grl.50303>, 2013.
- 30 Richter, A., Burrows, J. P., Nusz, H., Granier, C., and Niemeier, U.: Increase in tropospheric nitrogen dioxide over China observed from space, *Nature*, 437, 129–132, doi:10.1038/nature04092, <http://dx.doi.org/10.1038/nature04092>, 2005.
- Sharma, C., Tiwari, M. K., and Pathak: Estimates of emission and deposition of reactive nitrogenous species for India., *Current Science*, 94, 1439–1446, <http://npl.csircentral.net/1012/>, 2008.
- Sindelarova, K., Granier, C., Bouarar, I., Guenther, A., Tilmes, S., Stavrakou, T., Müller, J.-F., Kuhn, U., Stefani, P., and Knorr, W.: Global data set of biogenic VOC emissions calculated by the MEGAN model over the last 30 years, *Atmospheric Chemistry and Physics*, 14, 9317–9341, doi:10.5194/acp-14-9317-2014, <http://www.atmos-chem-phys.net/14/9317/2014/>, 2014.
- 35 Staehelin, J., Harris, N. R. P., Appenzeller, C., and Eberhard, J.: Ozone trends: A review, *Reviews of Geophysics*, 39, 231–290, doi:10.1029/1999RG000059, <http://dx.doi.org/10.1029/1999RG000059>, 2001.



- Steffen, W., Crutzen, P. J., and McNeill, J. R.: The Anthropocene: Are Humans Now Overwhelming the Great Forces of Nature, *AMBIO: A Journal of the Human Environment*, 36, 614–621, doi:10.1579/0044-7447(2007)36[614:TAAHNO]2.0.CO;2, [http://dx.doi.org/10.1579/0044-7447\(2007\)36\[614:TAAHNO\]2.0.CO;2](http://dx.doi.org/10.1579/0044-7447(2007)36[614:TAAHNO]2.0.CO;2), 2007.
- Stevenson, D. S., Dentener, F. J., Schultz, M. G., Ellingsen, K., van Noije, T. P. C., Wild, O., Zeng, G., Amann, M., Atherton, C. S., Bell, N., Bergmann, D. J., Bey, I., Butler, T., Cofala, J., Collins, W. J., Derwent, R. G., Doherty, R. M., Drevet, J., Eskes, H. J., Fiore, A. M., Gauss, M., Hauglustaine, D. A., Horowitz, L. W., Isaksen, I. S. A., Krol, M. C., Lamarque, J.-F., Lawrence, M. G., Montanaro, V., Müller, J.-F., Pitari, G., Prather, M. J., Pyle, J. A., Rast, S., Rodriguez, J. M., Sanderson, M. G., Savage, N. H., Shindell, D. T., Strahan, S. E., Sudo, K., and Szopa, S.: Multimodel ensemble simulations of present-day and near-future tropospheric ozone, *Journal of Geophysical Research: Atmospheres*, 111, n/a–n/a, doi:10.1029/2005JD006338, <http://dx.doi.org/10.1029/2005JD006338>, d08301, 2006.
- 5 Textor, C., Schulz, M., Guibert, S., Kinne, S., Balkanski, Y., Bauer, S., Bernsten, T., Berglen, T., Boucher, O., Chin, M., Dentener, F., Diehl, T., Easter, R., Feichter, H., Fillmore, D., Ghan, S., Ginoux, P., Gong, S., Grini, A., Hendricks, J., Horowitz, L., Huang, P., Isaksen, I., Iversen, I., Kloster, S., Koch, D., Kirkevåg, A., Kristjansson, J. E., Krol, M., Lauer, A., Lamarque, J. F., Liu, X., Montanaro, V., Myhre, G., Penner, J., Pitari, G., Reddy, S., Seland, Ø., Stier, P., Takemura, T., and Tie, X.: Analysis and quantification of the diversities of aerosol life cycles within AeroCom, *Atmospheric Chemistry and Physics*, 6, 1777–1813, doi:10.5194/acp-6-1777-2006, <http://www.atmos-chem-phys.net/6/1777/2006/>, 2006.
- 10 Tsigaridis, K., Krol, M., Dentener, F. J., Balkanski, Y., Lathière, J., Metzger, S., Hauglustaine, D. A., and Kanakidou, M.: Change in global aerosol composition since preindustrial times, *Atmospheric Chemistry and Physics*, 6, 5143–5162, doi:10.5194/acp-6-5143-2006, <http://www.atmos-chem-phys.net/6/5143/2006/>, 2006.
- Tsigaridis, K., Daskalakis, N., Kanakidou, M., Adams, P. J., Artaxo, P., Bahadur, R., Balkanski, Y., Bauer, S. E., Bellouin, N., Benedetti, A., Bergman, T., Bernsten, T. K., Beukes, J. P., Bian, H., Carslaw, K. S., Chin, M., Curci, G., Diehl, T., Easter, R. C., Ghan, S. J., Gong, S. L., Hodzic, A., Hoyle, C. R., Iversen, T., Jathar, S., Jimenez, J. L., Kaiser, J. W., Kirkevåg, A., Koch, D., Kokkola, H., Lee, Y. H., Lin, G., Liu, X., Luo, G., Ma, X., Mann, G. W., Mihalopoulos, N., Morcrette, J.-J., Müller, J.-F., Myhre, G., Myriokefalitakis, S., Ng, N. L., O'Donnell, D., Penner, J. E., Pozzoli, L., Pringle, K. J., Russell, L. M., Schulz, M., Sciare, J., Seland, Ø., Shindell, D. T., Sillman, S., Skeie, R. B., Spracklen, D., Stavroukou, T., Steenrod, S. D., Takemura, T., Tiitta, P., Tilmes, S., Tost, H., van Noije, T., van Zyl, P. G., von Salzen, K., Yu, F., Wang, Z., Wang, Z., Zaveri, R. A., Zhang, H., Zhang, K., Zhang, Q., and Zhang, X.: The AeroCom evaluation and intercomparison of organic aerosol in global models, *Atmospheric Chemistry and Physics*, 14, 10 845–10 895, doi:10.5194/acp-14-10845-2014, <http://www.atmos-chem-phys.net/14/10845/2014/>, 2014.
- 20 van der A, R. J., Allaart, M. A. F., and Eskes, H. J.: Multi sensor reanalysis of total ozone, *Atmospheric Chemistry and Physics*, 10, 11 277–11 294, doi:10.5194/acp-10-11277-2010, <http://www.atmos-chem-phys.net/10/11277/2010/>, 2010.
- 30 van Vuuren, D., Edmonds, J., Kainuma, M., Riahi, K., and Weyant, J.: A special issue on the RCPs, *Climatic Change*, 109, 1–4, doi:10.1007/s10584-011-0157-y, <http://dx.doi.org/10.1007/s10584-011-0157-y>, 2011.
- Vignati, E., Facchini, M., Rinaldi, M., Scannell, C., Ceburnis, D., Sciare, J., Kanakidou, M., Myriokefalitakis, S., Dentener, F., and O'Dowd, C.: Global scale emission and distribution of sea-spray aerosol: Sea-salt and organic enrichment, *Atmospheric Environment*, 44, 670 – 677, doi:<http://dx.doi.org/10.1016/j.atmosenv.2009.11.013>, <http://www.sciencedirect.com/science/article/pii/S1352231009009571>, 2010.
- 35 Vingarzan, R.: A review of surface ozone background levels and trends, *Atmospheric Environment*, 38, 3431 – 3442, doi:<http://dx.doi.org/10.1016/j.atmosenv.2004.03.030>, <http://www.sciencedirect.com/science/article/pii/S1352231004002808>, 2004.
- Volz, A. and Kley, D.: Evaluation of the Montsouris series of ozone measurements made in the nineteenth century, *Nature*, 332, 240–242, doi:10.1038/332240a0, <http://dx.doi.org/10.1038/332240a0>, 1988.



- Wang, R., Tao, S., Shen, H., Huang, Y., Chen, H., Balkanski, Y., Boucher, O., Ciais, P., Shen, G., Li, W., Zhang, Y., Chen, Y., Lin, N., Su, S., Li, B., Liu, J., and Liu, W.: Trend in Global Black Carbon Emissions from 1960 to 2007, *Environmental Science & Technology*, 48, 6780–6787, doi:10.1021/es5021422, <http://dx.doi.org/10.1021/es5021422>, PMID: 24825392, 2014.
- West, J. J., Smith, S. J., Silva, R. A., Naik, V., Zhang, Y., Adelman, Z., Fry, M. M., Anenberg, S., Horowitz, L. W., and Lamarque, J.-F.:
5 Co-benefits of mitigating global greenhouse gas emissions for future air quality and human health, *Nature Clim. Change*, 3, 885–889, <http://dx.doi.org/10.1038/nclimate2009>, letter, 2013.
- Worden, H. M., Deeter, M. N., Frankenberg, C., George, M., Nichitiu, F., Worden, J., Aben, I., Bowman, K. W., Clerbaux, C., Coheur, P. F.,
de Laat, A. T. J., Detweiler, R., Drummond, J. R., Edwards, D. P., Gille, J. C., Hurtmans, D., Luo, M., Martínez-Alonso, S., Massie,
S., Pfister, G., and Warner, J. X.: Decadal record of satellite carbon monoxide observations, *Atmospheric Chemistry and Physics*, 13,
10 837–850, doi:10.5194/acp-13-837-2013, <http://www.atmos-chem-phys.net/13/837/2013/>, 2013.
- Yoon, J. and Pozzer, A.: Model-simulated trend of surface carbon monoxide for the 2001–2010 decade, *Atmospheric Chemistry and Physics*,
14, 10 465–10 482, doi:10.5194/acp-14-10465-2014, <http://www.atmos-chem-phys.net/14/10465/2014/>, 2014.
- Zhang, J. and Reid, J. S.: A decadal regional and global trend analysis of the aerosol optical depth using a data-assimilation grade over-water
MODIS and Level 2 MISR aerosol products, *Atmospheric Chemistry and Physics*, 10, 10 949–10 963, doi:10.5194/acp-10-10949-2010,
15 <http://www.atmos-chem-phys.net/10/10949/2010/>, 2010.



Table 1. Statistics of comparison of model (CL simulation) vs. observations and fine resolution simulation (CL-fine) vs. observations (corresponding to pollutant concentration scatter plots shown in Fig. 3 and Fig. S2). #pairs shows the number of pairs used for the comparison, meas and model are mean of all gridded data that are used for the comparisons (as described in section 3.2). NMB stands for normalized mean bias of the model against the measurements. C stands for the CL simulation ($6^\circ \times 4^\circ$) and F stands for the CL-fine simulation ($3^\circ \times 2^\circ$). The units are ppb for gases (O_3 , CO) and $\mu g m^{-3}$ for aerosols (SO_4^{2-} , OC, BC, NH_4^+).

	#pairs		meas		model		R		NMB* (%)	
	C	F	C	F	C	F	C	F	C	F
O_3	1555	2417	30.86	31.08	34.89	36.32	0.46	0.48	13	17
CO	211	229	149.24	149.87	151.64	148.62	0.42	0.41	2	-1
SO_4^{2-}	2008	3592	2.57	2.51	3.91	4.04	0.74	0.71	52	61
OC	1037	1825	3.24	2.92	1.25	1.22	0.59	0.71	-62	-57
BC	931	1728	0.29	0.28	0.28	0.29	0.59	0.50	-3	1
NH_4^+	626	777	0.94	0.92	2.24	2.30	0.65	0.64	140	149

*Normalized mean bias is calculated as: $NMB = \frac{\sum(M_i - O_i)}{\sum O}$ where M stands for Model and O for Observations

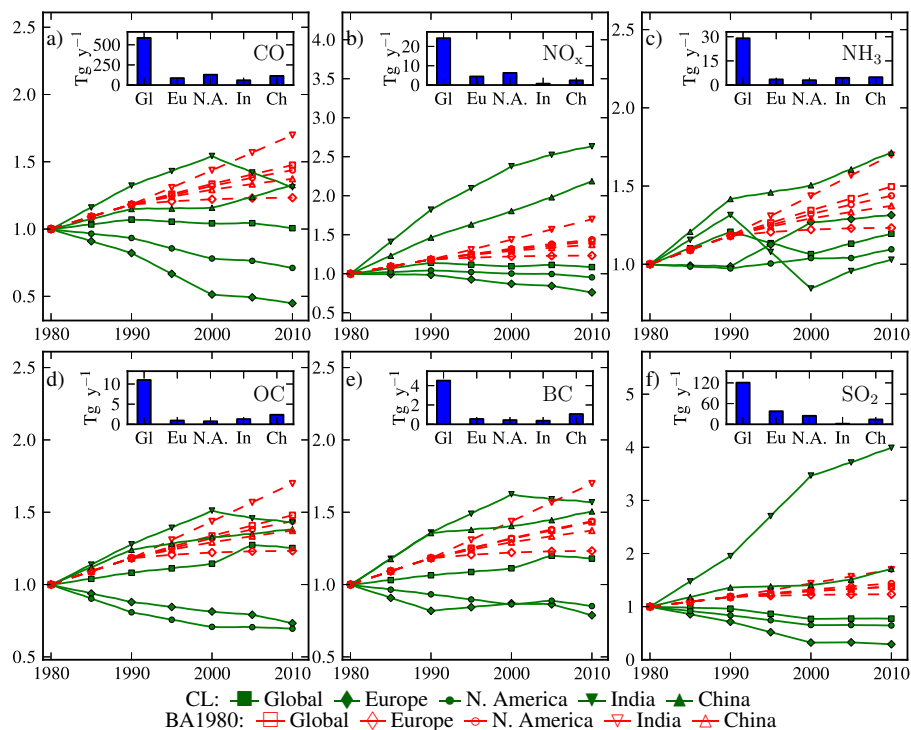


Figure 1. Normalized (to 1980 levels) annual mean anthropogenic emissions of CO, NO_x, NH₃, OC, BC and SO₂ for the CL (green/solid) and BA1980 (red/dashed) simulations as a function of time. Different regions appear with different symbols: squares for the globe (Gl), diamonds for Europe (Eu), triangles for China (Ch), inverted triangles for India (In), and circles for North America (N.A.). The histograms at the top of each panel show the absolute emissions in 1980 (used to normalize the emissions) for these regions that are used as reference to normalize emissions (also shown in Table S1).

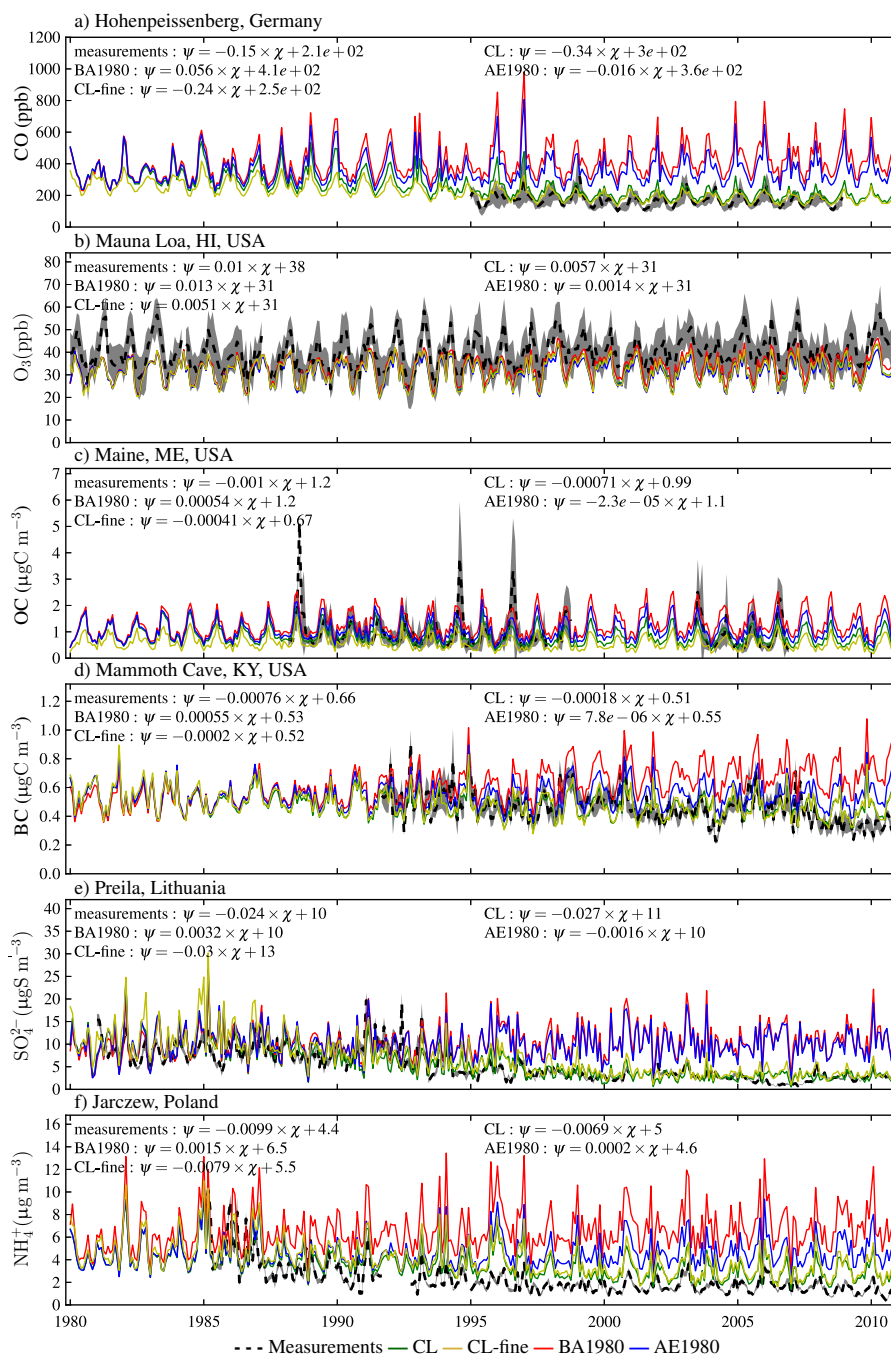


Figure 2. Comparison of the four simulations against observations. The dashed line and shadowed areas indicate monthly mean surface observations and one standard deviation. Simulations are CL: current legislation (green); CL-fine: current legislation in the fine resolution of the model; BA1980: Business As in 1980, with constant anthropogenic emission rates per capita as in 1980 (red); AE1980: constant anthropogenic emissions as in 1980 (blue). Trends derived from the concentrations (ψ) as a function of the year (χ) are provided for the measurements and the four simulations inside the frames.

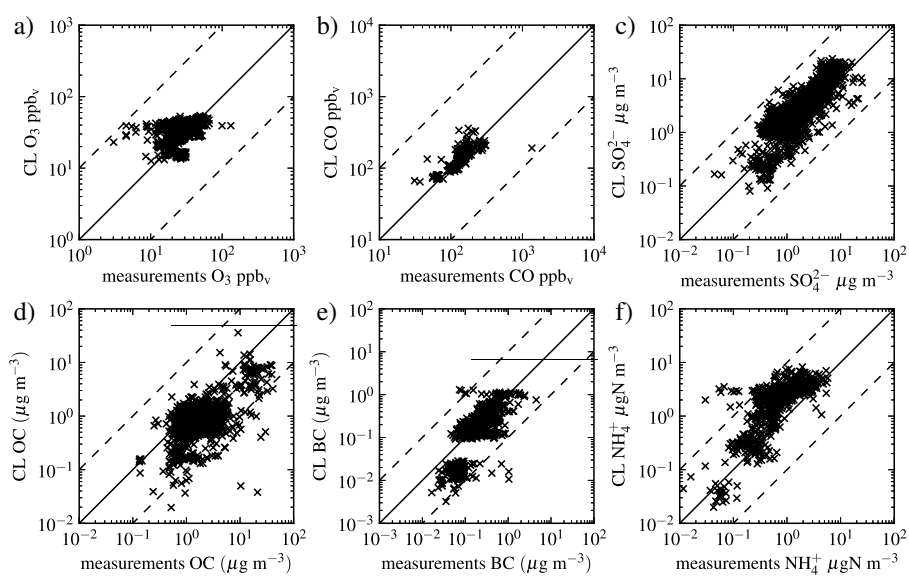


Figure 3. Comparisons of annual average surface model results versus observations per model grid (see Fig. S5 for station locations) a) for O_3 , b) for CO, c) for SO_4^{2-} , d) for OC, e) for BC, f) NH_4^+ . The continuous line denotes the 1:1 slope and the dashed lines the 10:1 and 1:10 slopes

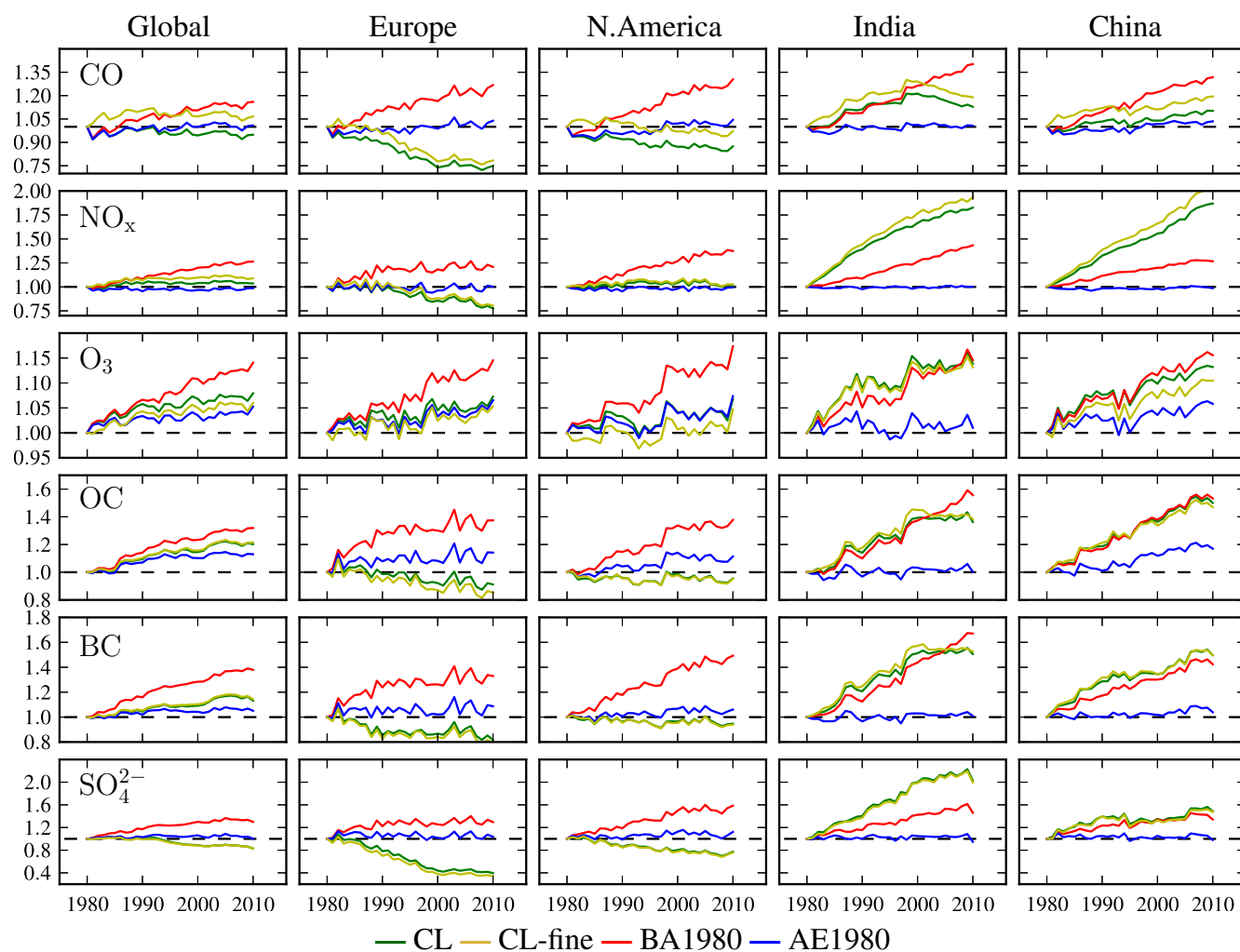


Figure 4. Normalized annual mean surface concentrations for CO, NO_x, O₃, OC, BC, and sulphate aerosols (rows), averaged over the globe, Europe, North America, India and China (columns). The difference between the blue (AE1980) and green (CL) lines is the anticipated change in concentrations when assuming 1980 anthropogenic emissions at any given year, while the difference between the red (BA1980) and green (CL) lines is the calculated change in concentrations at any given year when taking into account the increased anthropogenic emissions due to the population growth. The yellow lines depict the annual mean surface concentrations of the CL-fine simulation. Note the difference in scales between species.